Structure and High-Temperature Oxidation Properties of an Al-Co-Y diffusion Coating prepared on TiAl-Nb alloy at a Low Temperature

Xuan Li *, Zekun Wei , Wei Lv , Lijing Zhang , Fuhua Liu , Xiaoqing Xie , Sheng Lai , Xuyi Zhang

Posted Date: 5 September 2023

doi: 10.20944/preprints202309.0273.v1

Keywords: TiAl alloy; Pack cementation; Coating structure; Coating formation process; High-temperature oxidation

Article

Structure and High-Temperature Oxidation Properties of an Al-Co-Y Diffusion Coating Prepared on TiAl-Nb Alloy at a Low Temperature

Xuan Li [1,*], Zekun Wei [1], Wei Lv [1], Lijing Zhang [2], FuHua Liu [3], Xiaoqing Xie [1,4], Xuyi Zhang [1] and Sheng Lai [1]

[1] College of Mechanical Engineering, Sichuan University of Science and Engineering, Zigong, 643000, Sichuan, China
[2] China United Northwest Institute for Engineering Design and Research Corporation, Xi'an, 710077, China
[3] School of automobile and rail transit, Yibin Vocational and Technical College, Yibin, 644003, Sichuan, China
[4] College of Mechanical Engineering, Sichuan Vocational College of Chemical Industry, Luzhou 6460992, China;
* Correspondence: biluaner@163.com; Tel.:+86-135-5076-3677

Abstract: An Al-Co-Y diffusion coating was prepared on a TiAl alloy by pack cementation process at a low temperature range of 650-720 ℃. The influence of different activators and co-deposition temperatures on the coating's microstructure and formation process, and high temperature oxidation performance was studied. The results showed that NaF was a more suitable activator for preparing the Al-Co-Y diffusion coating on TiAl alloy compared to NH_4Cl and $AlCl_3$. A more compact coating structure can be obtained when deposition was performed at 680 ℃ using NaF as the activator. The coating was mainly composed of a $TiAl_3$ outer layer, a $TiAl_2$ inner layer, and a thin Al-rich TiAl inter-diffusion layer. The growth of the coating exhibited a positive linear correlation between coating thickness increase and the square root of deposition time. The high-temperature oxidation tests showed that a dense scale mainly composed of Al_2O_3 and a small amount of TiO_2 formed on the coating after oxidation at 950 ℃ for 100 h. The scale possessed excellent high-temperature oxidation resistance, with a parabolic rate constant of the oxidation weight gain approximately 4.9×10^{-3} mg^2/cm^4 h, which is lower than that of the TiAl substrate by about three orders of magnitude, and lower than that of the pure Al diffusion coating more than one order of magnitude.

Keywords: TiAl alloy; pack cementation; Al-Co-Y diffusion coating; coating structure; high-temperature oxidation

1. Introduction

Due to the advantages of low density, high strength and specific strength, high modulus, and outstanding high-temperature mechanical properties, γ-TiAl alloys hold promising application prospects in aircraft engines and gas turbines [1]. However, the high-temperature oxidation resistance of TiAl alloys needs further improvement. The high activity of Ti and the internal oxidation of Al hinder the formation of a single Al_2O_3 protective film on TiAl alloys during high-temperature oxidation; as a result, a large amount of poorly protective TiO2 forms in the scale and consequently weakens the high-temperature oxidation resistance of the alloys [2]. Therefore, further enhancement in anti-oxidation performance of TiAl alloys is necessary for their components serving in high-temperatures.

Alloying and preparing surface protective coatings have been demonstrated to be the effective ways to enhance the high temperature oxidation resistance of TiAl alloys. Regarding alloying, the addition of a high Nb content can lead to a significantly improvement to the strength and high-

 doi:10.20944/preprints202309.0273.v1

temperature oxidation resistance of TiAl alloys without obviously reducing their room-temperature plasticity [3]. Alloying with elements such as Mo [4], W [5], Si [6], Cr [7], Ta [8], or trace rare earth elements such as Ce [9] and Y [10], can also be used to promote the formation of protective Al_2O_3, suppress internal oxidation and delay the degradation of oxide films. However, the incorporation of a large amount of elements that enhance the oxidation resistance of TiAl alloys may potentially weaken their mechanical properties or other properties.

Preparation of oxidation-resistant coatings can enhance the high-temperature oxidation resistance of TiAl alloys effectively, while causing less degradation to their mechanical properties. In past decades, researchers have investigated various antioxidant coatings for TiAl alloys. These coatings include aluminide coatings ($TiAl_3$, $TiAl_2$, etc.) [11–13], TiAlCr coatings [14,15], M-CrAlY (M = Ni, Co, or NiCo) coatings [16,17], ceramic coatings [18–20], silicide coatings [21,22], and a variety of composite coatings. Among them, aluminide coatings can form a dense Al_2O_3 protective film when oxidation at high temperatures. Moreover, the well matched thermal expansion coefficients between the aluminide coatings and TiAl alloys can prevent cracking or spalling during cooling/heating process, thereby resulting in outstanding high-temperature oxidation resistance. However, the inherent brittleness of aluminide coatings, combined with significant Ti and Al inter-diffusion at high temperatures between the coatings and the TiAl substrate, accelerates the degradation and eventual failure of the coatings. TiAlCr coatings and MCrAlY coatings can form a composite oxide film consisting of Al_2O_3/Cr_2O_3 at high temperatures, and the Cr-rich inner layer inhibits the elemental inter-diffusion between the coating and substrate alloy, thereby retarding the failure of the coating [23,24]. Particularly, MCrAlY coatings, utilizing the reactive element effect (REE) generated by trace rare earths in the coating, exhibit improved adhesion, thermal fatigue properties, and greater flexibility in composition choice. As a result, these coatings have broad applications in high-temperature alloys [25]. However, these coatings are not suitable for use as protective coatings for γ-TiAl due to the poor compatibility between the coating and the substrate [26].

Pack cementation is an improved chemical vapor deposition technique with simple equipment requirements, low cost, and high flexibility of substrate. It can be used to easily prepare aluminide or modified aluminide coatings with stable and dense structures and strong metallurgical bonds on TiAl alloys. These features are beneficial for TiAl alloy components such as engine blades and vortex generators that need to withstand complex loads. At present, aluminides [27], silicides [28], Al-Cr [29–31], Al-Si [32,33], and their rare-earth-modified composite coating systems have been successfully prepared on TiAl alloys by this method. However, most of these coatings have been reported to be prepared at high-temperatures, thus the preparation process can impose adverse effects on the comprehensive mechanical properties of TiAl substrates. In addition, due to the low activity of Co and the poor reactivity between Co and the TiAl matrix, rare-earth-modified Al-Co composite coatings and their antioxidant properties have rarely been reported.

In this paper, an Al-Co-Y diffusion coating was prepared on a TiAl alloy using pack cementation method at a low-temperature range of 650-720 ℃. The effect of the activator, co-deposition temperature, and deposition time on the microstructure of the coating was studied, and the high-temperature oxidation resistance of the coating with optimized microstructure was tested. The main objective of this research is to develop a protective coating for TiAl alloys that possesses a dense structure, strong adhesion to the matrix, and superior anti-oxidation performance at high temperatures.

2. Materials and Methods

The employed TiAl substrate has a composition of Ti-45Al-8Nb-0.1Y (at.%), which was prepared by vacuum arc non-self-consuming melting method. Cuboid specimens with a size of 5 mm × 5 mm × 3 mm were cut from the melted alloy ingots using electrical discharge machining (EDM). The surface of each specimen was polished using 400 # - 1000 # SiC sandpaper step by step, and then ultrasonically cleaned in alcohol for 10 min, and blown dry by cold air.

The Al-Co-Y diffusion coatings were prepared using a GF17Q-I high-temperature furnace. The pack powder composition was chosen as 20Al-10Co-2Y-5M-63Al_2O_3 (wt.%), where Al, Co, and Y

Preprints (www.preprints.org) | NOT PEER-REVIEWED | Posted: 5 September 2023 doi:10.20944/preprints202309.0273.v1

were the co-deposited elements, M was the activator (M = NaF, NH_4Cl, or $AlCl_3$), and Al_2O_3 was the filler. Each group of powders was accurately weighed, and then ground in a planetary ball mill for 4 h to make them fully mixed and refined.

The coating preparation process was as follows: First, the specimen was buried in an alumina crucible with the powder. Then the crucible was sealed with Al_2O_3 and silica sol and placed in a high-temperature furnace, and the furnace was heated from room temperature to the deposition temperatures of 650-720 ℃ with a heating rate of 10 ℃/min and then held for 2-10 h. After coating, the surfaces of the samples was slightly brushed using a soft bristle brush, and then ultrasonically cleaned in an acetone bath to remove the residual pack powders.

High-temperature oxidation experiments of the Al-Co-Y diffusion coating with an optimized structure were carried out in a SX2-2.5-12A muffle furnace at 950℃ for 1 h, 10 h, 50 h, and 100 h. During oxidation, the specimens were placed in corundum crucibles that had been heated until no change in mass was observed, in order to collect any flaked-off oxidation products. In order to make a comparison, oxidation tests were also performed on the pure Al diffusion coating, which was prepared using the same deposition parameters as the optimized Al-Co-Y diffusion coating.

The mass changes of the specimens before and after oxidation were measured by an electronic balance with an accuracy of 0.1 mg. To reduce weighing errors, each specimen was measured for five times. X-ray diffraction (XRD) was employed to determine the phase composition of the coating and oxide film, and scanning electron microscopy (SEM; JSM-6360LV) equipped with energy-dispersive spectroscopy (EDS) were used to analyze the micromorphology and chemical composition of the specimens before and after oxidation.

3. Results

3.1. Structure of the Al-Co-Y diffusion coating

3.1.1. Effects of activators

Figure 1 shows the cross-sectional morphology of the Al-Co-Y diffusion coatings prepared on the TiAl alloy at 680 ℃ for 6 h, with using NH_4Cl, $AlCl_3$ and NaF as the activators All the obtained coatings are well bonded to the substrate. The coating prepared with NH_4Cl was about 25 μm thick, and the entire coating was loose with many holes formed inside. The coating prepared with $AlCl_3$ is more compact than the coating prepared with NH_4Cl, but there were also numerals holes and cracks formed. The coating prepared with NaF is about 17 μm thick, and is the most compact one among the three coatings.

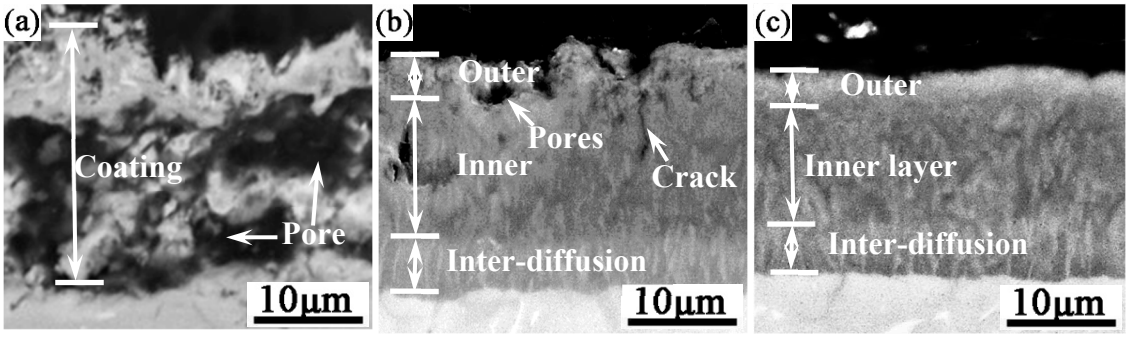

Figure 1. Cross-sectional backscattered electron (BSE) images of the Al-Co-Y diffusion coatings prepared at 680 ℃ for 6 h using different activators: (a) NH_4Cl; (b) $AlCl_3$; (c) NaF.

The XRD patterns in Figure 2 show that the outer layers of the coatings prepared with all three activators were mainly composed of $TiAl_3$, but weak $TiAl_2$-phase diffraction peaks appeared in the pattern of the coating prepared with $AlCl_3$. EDS analysis determined that the outer layers of the three coatings have mean compositions of 18.22Ti-63.45Al-17.86Nb-0.43Co-0.03Y (at.%), 16.82Ti-65.35Al-17.58Nb-0.21Co-0.04Y (at.%), and 16.85Ti-65.87Al-16.91Nb- 0.32Co-0.05Y (at.%) for activators of

Preprints (www.preprints.org) | NOT PEER-REVIEWED | Posted: 5 September 2023 doi:10.20944/preprints202309.0273.v1

respectively NH_4Cl, $AlCl_3$ and NaF. Obviously, the EDS analysis results also confirm the formation of $TiAl_3$ outer layers of teach coating. The atomic ratios of Ti and Al in the inner layers and the inter-diffusion layers of the coating prepared with different activators were approximately 1:2 and 1:1, respectively. Combined with the Ti-Al-Nb ternary phase diagram [34], the inner layers were mainly $TiAl_2$, and the inter-diffusion layers were mainly Al rich γ-TiAl. From the perspective of the coating structure and phase composition, NaF was more suitable than NH_4Cl and $AlCl_3$ for preparing Al-Co-Y diffusion coatings on TiAl alloy at a low temperature of 680 ℃.

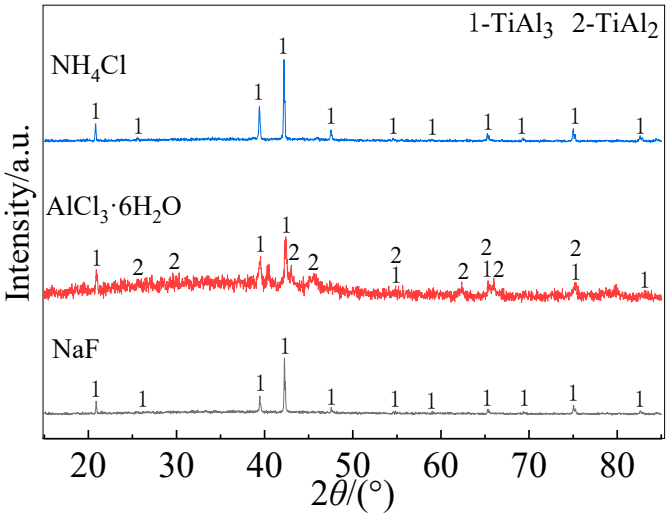

Figure 2. Surface XRD patterns of the Al-Co-Y diffusion coatings prepared at 680 ℃ for 6 h using different activators.

3.1.2. Effects of co-deposition temperatures

Figure 3 shows the backscattered electron (BSE) morphology and elemental distribution along the depth-direction of the Al-Co-Y diffusion coatings prepared by using NaF as the activator at 650 ℃, 680 ℃ and 720 ℃ for 10 h. Figure 4 shows the XRD patterns of each coating surface. The coatings prepared at different temperatures had similar structures, consisting of an outer layer, an inner layer, and an inter-diffusion layer, but the thickness and density of the coatings were different.

Preprints (www.preprints.org) | NOT PEER-REVIEWED | Posted: 5 September 2023 doi:10.20944/preprints202309.0273.v1

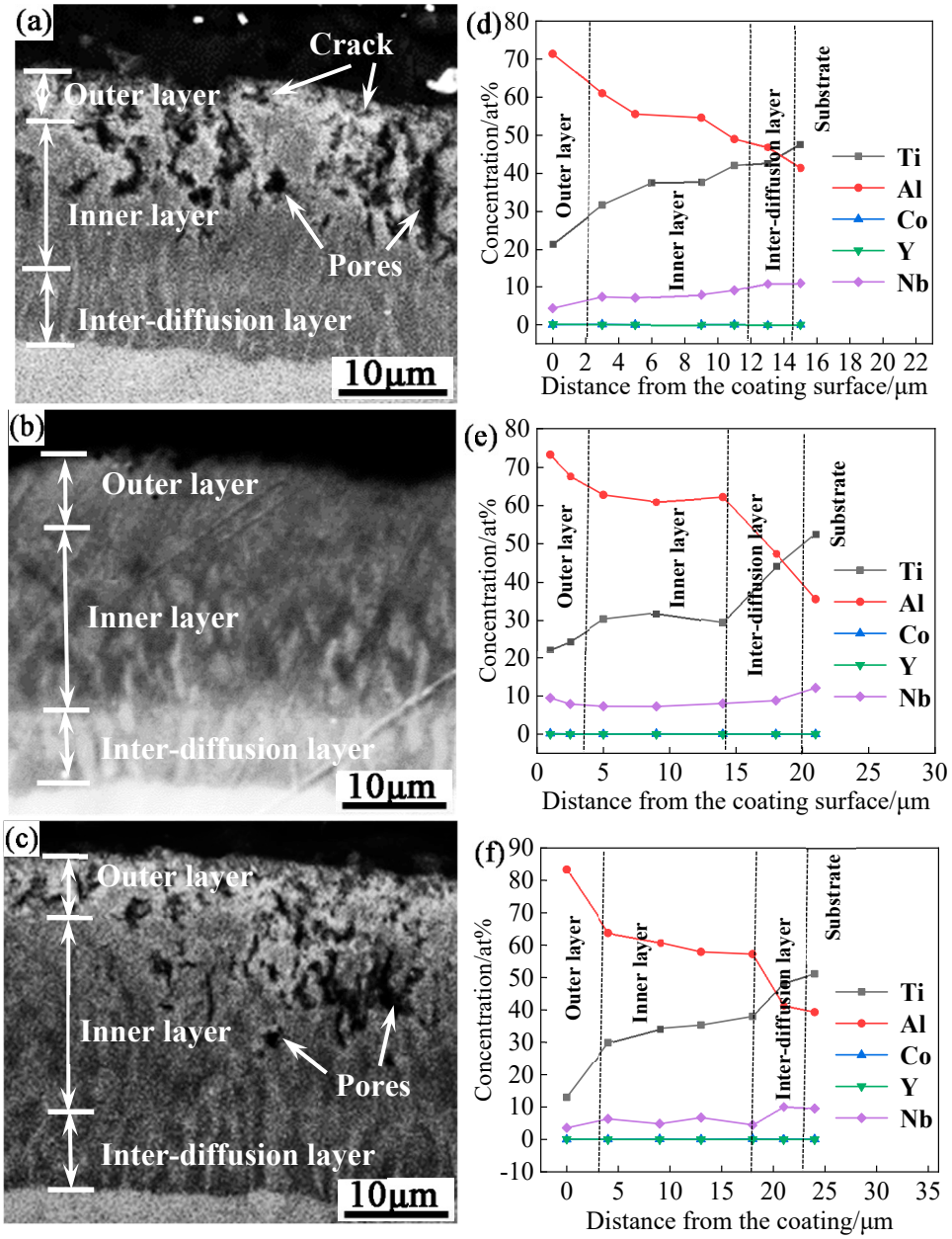

Figure 3. Cross-sectional BSE images (a), (b), (c) and elemental concentration profiles (d), (e), (f) of the Al-Co-Y diffusion coatings prepared at temperatures of (a) (d) 650 ℃, (b) (e) 680 ℃, and (c) (f) 720 ℃ for 6 h.

Preprints (www.preprints.org) | NOT PEER-REVIEWED | Posted: 5 September 2023 doi:10.20944/preprints202309.0273.v1

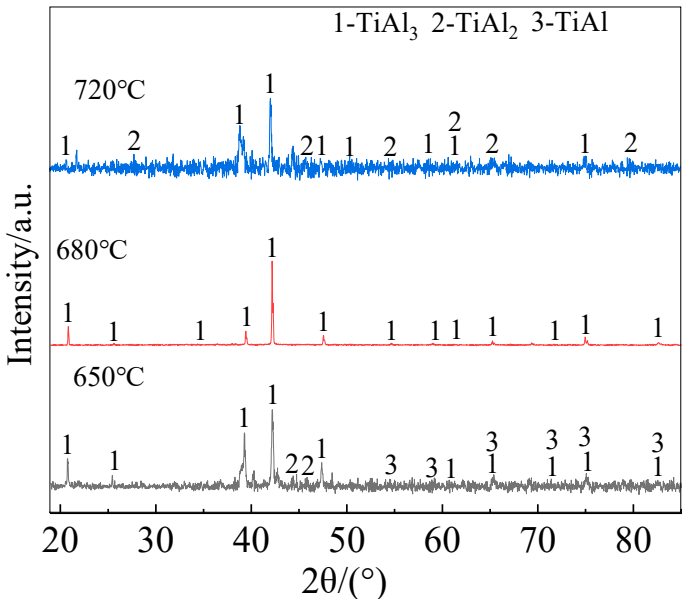

Figure 4. Surface XRD patterns of the Al-Co-Y diffusion coatings prepared at 650 °C, 680 °C and 720 °C for 10 h.

As seen in Figure 3(a), the coating prepared at 650 °C has a thickness about 15 μm, with an outer layer measuring about 2 μm, an inner layer about 10 μm, and an inter-diffusion layer about 3 μm. Numerous pores and cracks were present in both the outer and inner layers. Combining the EDS composition analysis in Figure 3(d), XRD analysis in Figure 4, and Ti-Al-Nb ternary phase diagram [34], the outer layer was determined to be mainly composed of $TiAl_3$ and a small amount of TiAl. The atomic percentages of Ti and Al in the inner layer and the inter-diffusion layer were about 1: 2 and 1: 1, respectively. Combined with the Ti-Al-Nb ternary phase diagram [34], the inner layer was determined as $TiAl_2$, and the inter-diffusion layer was composed of Al-rich γ-TiAl phase.

The coating prepared at 680 °C was dense and well bonded to the substrate. The coating has an overall thickness of about 20 μm, with an outer layer about 5 μm, an inner layer about 11 μm, and an inter-diffusion layer about 4 μm, as shown in Figure 3(b). The EDS composition analysis in Figure 3(e) show that the typical composition of the outer layer was 17.13 Ti-73.20 Al-9.47 Nb-0.19 Co-0.01 Y (at.%). Combined with the XRD pattern in Figure 4 and the Ti-Al-Nb ternary phase diagram [34], the outer layer was mainly composed of $TiAl_3$ phase. The atomic ratios of Ti and Al in the inner layer and the inter-diffusion layer were about 1: 2 and 1: 1, respectively. Combined with the Ti-Al-Nb ternary phase diagram [34], the inner layer was mainly composed of $TiAl_2$, while the inter-diffusion layer was mainly composed of Al-rich γ-TiAl. Additionally, distinctive light-colored tissues can be found in both the inner layer and inter-diffusion layer, because these tissues were higher in Nb content compared to the dark phase.

The coating prepared at 720 °C has a total thickness of about 24 μm, with an outer layer around 3 μm, an inner layer around 16 μm, and an inter-diffusion layer approximately 5 μm. Numerous pores formed in the coating. The EDS composition analysis and surface XRD analysis indicated that the coating prepared at 720 °C also mainly consisted of a $TiAl_3$ outer layer, a $TiAl_2$ inner layer, and a TiAl inter-diffusion layer. However, a small amount of $TiAl_2$ phase was formed in the outer layer of the coating.

3.1.2. Growth kinetics of the coating prepared at 680 °C

Figure 5 shows the growth kinetic curves and BSE morphologies of the cross-sectional structure of the Al-Co-Y diffusion coatings prepared at 680 °C for 2-10 h. Figure 6 shows the surface XRD patterns of the coatings prepared for different holding time. Both the total thickness of the coating and the thickness of each layer within the coating increased significantly with prolonging the holding time. The fitted curve in Figure 5 illustrates the relationship between the coating thickness and the

Preprints (www.preprints.org) | NOT PEER-REVIEWED | Posted: 5 September 2023 doi:10.20944/preprints202309.0273.v1

square root of the holding time. It is seen that the growth kinetics of the Al-Co-Y diffusion coating at 680 ℃ followed a parabolic law, i.e., there is a positive linear correlation between the increase in coating thickness and the square root of deposition time. This indicates that the growth of the coating was controlled by the inward diffusion of Al, Co, and Y in the TiAl matrix. In addition, from the cross-sectional BSE morphologies of the coating in Figure 5 and the surface XRD patterns in Figure 6, it can be seen that the outer layers of the coatings prepared for different holding time were mainly composed of $TiAl_3$ phase; however, small amount of $TiAl_2$ formed at the initial stage of co-deposition (2 h). With prolonging the co-deposition to 4 h, the diffraction peaks from $TiAl_2$ phase disappeared, indicating that the formation of $TiAl_2$ phase was preferred to $TiAl_3$ during the coating formation process.

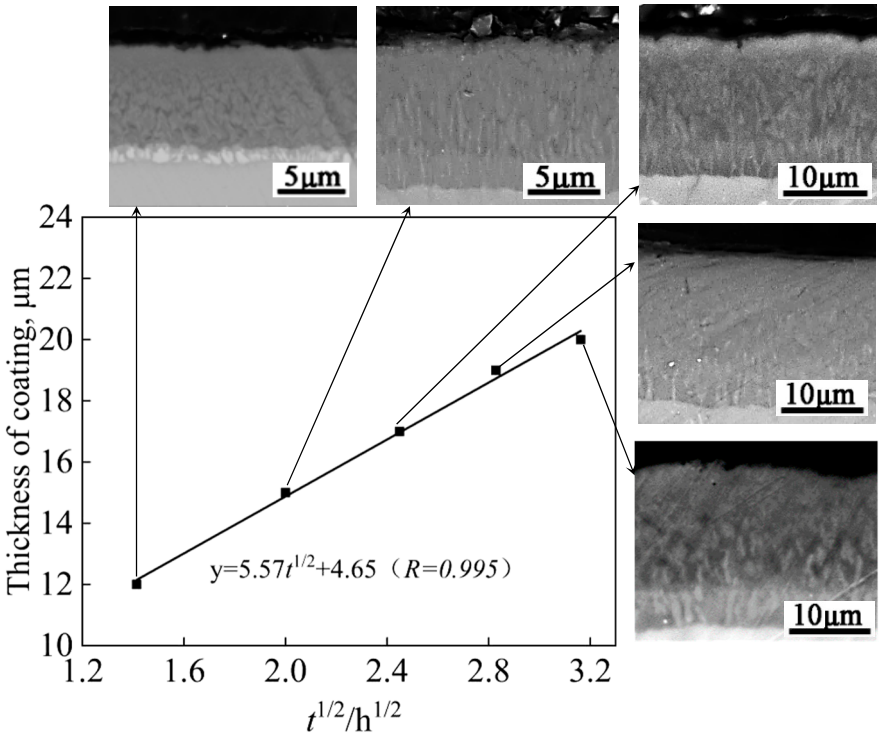

Figure 5. Growth kinetics and cross-sectional BSE images of the Al-Co-Y diffusion coatings prepared at 680 ℃.

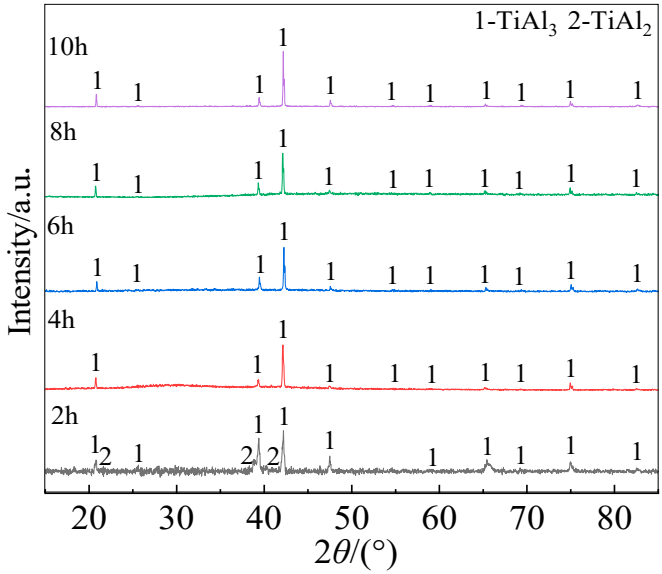

Preprints (www.preprints.org) | NOT PEER-REVIEWED | Posted: 5 September 2023 doi:10.20944/preprints202309.0273.v1

Figure 6. Surface XRD patterns of the Al-Co-Y diffusion coatings prepared at 680 °C for different time.

3.2. *Formation of the coating structure*

The formation of the coating is closely related to the generation and transport of the active atoms of the deposited elements in the pack and their inward diffusion or reactive diffusion in the substrate [35]. This process can be generally described as follows: The gas-phase halides of the co-deposited elements that produced by reactions of the activator and deposited elements, will gradually diffuse onto the surface of the substrate, and then underwent interfacial phase reactions such as decomposition, substitution, or disproportionation to form the coating [36]. The experimental results in this paper indicate that the Al-Co-Y diffusion coating prepared on TiAl alloy was mainly composed of aluminides, with low concentrations of Co and Y. This suggests that the inward diffusion of Al played a significant role for the formation of the coating. The development of a diffusion coating was also closely related to the activity of the deposited atoms and their reactivity with the base alloy. In the co-deposition system, the reactivity between Al-Ti at high temperatures was higher than that between Co-Ti and Y-Ti. It is a reaction system with a lower Gibbs free energy, so the formation of the coating is dominated by the reactive diffusion of Al and Ti, and Co and Y mainly entered the coating via concentration-driven diffusion. The melting points of Co and Y are 1768 K and 1799 K, respectively. According to the empirical equation $Q = 32T_m$ (where Q is the diffusion activation energy of the substance, and T_m is the melting point of the substance) [37], the diffusion activation energy required for Co and Y is higher, resulting in lower diffusion coefficients. Therefore, the inward diffusion rate of Co and Y atoms is slower at the temperatures examined in this paper.

The relationship between the free energy magnitudes of TiAl, $TiAl_2$, and $TiAl_3$ formation in the temperature range of 273 to 1473 K followed an order of $\Delta G(TiAl) > \Delta G(TiAl_3) > \Delta G(TiAl_2)$ [38,39]. Therefore, the reactive diffusion of active Al atoms in the matrix alloy predominantly formed $TiAl_2$ phase (reaction (3) and Figure 7(a)). Wang [40] and Gleeson [21] calculated the intrinsic rate constants, K_p, for the formation of $TiAl_3$ and $TiAl_2$ during the growth of the coating as:

$$K_p(TiAl_2)=K'_p(TiAl_2)(1+3V_1X_2/2V_2X_1) \quad (1)$$

$$K_p(TiAl_3)=K'_p(TiAl_3)(1+V_2X_1/V_1X_2) \quad (2)$$

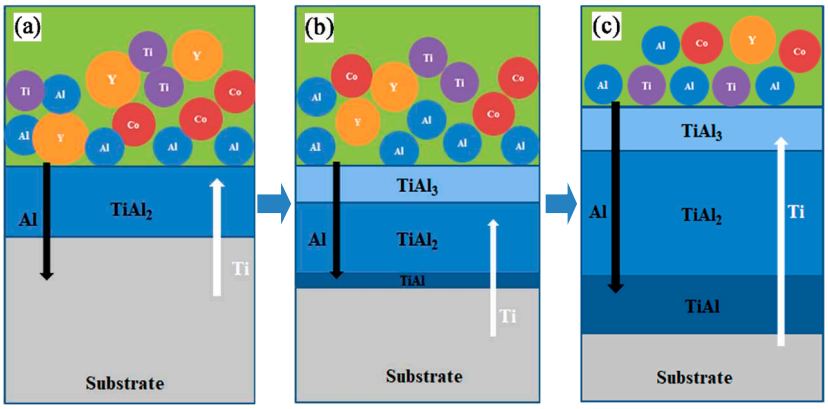

Figure 7. Schematic diagram of the coating formation process.

The intrinsic rate constants of $TiAl_2$ and $TiAl_3$ were calculated to be 6.9 and 18.9 $\mu m \cdot h^{-1/2}$, respectively, demonstrating that the diffusion rate of Al atoms in $TiAl_3$ was higher than that in in $TiAl_2$. As a result, a large number of active Al atoms accumulated on the surface of $TiAl_2$, reacting with outward-diffusing Ti atoms to form $TiAl_3$ layer (as shown by the reaction equation (4)). During the growth of the $TiAl_3$ layer, some $TiAl_3$ also reacted with the out-diffused Ti atoms to form $TiAl_2$ (as shown in equation (5)) [41]. There was a relationship between the magnitude of the generation free energy of $TiAl_2$ and $TiAl_3$, as the main $TiAl_2$ generation reaction also continued (as shown in equation (3)). Combining the above reactions, the overall growth rate of $TiAl_2$ in the coating prepared

Preprints (www.preprints.org) | NOT PEER-REVIEWED | Posted: 5 September 2023 doi:10.20944/preprints202309.0273.v1

in this paper was greater than that of $TiAl_3$. Near the coating/substrate alloy interface, the internal diffusion of active [Al] atoms promoted the formation of an Al-rich γ-TiAl inter-diffusion layer. At this diffusion stage, the fundamental structure of the coating began to take shape,, as shown in Figure 7.

$$Ti + 2[Al] \rightarrow TiAl_2 \quad (3)$$

$$Ti + 3[Al] \rightarrow TiAl_3 \quad (4)$$

$$Ti + 2TiAl_3 \rightarrow 3TiAl_2 \quad (5)$$

$$Ti + [Al] \rightarrow TiAl \quad (6)$$

As diffusion continued, TiAl, $TiAl_2$, and $TiAl_3$ layers became thicker, with the $TiAl_2$ layer being the thickest because of its fastest growth rate. At the later stage of diffusion, the large consumption of active Al atoms led to an insufficient supply resource, and the vacancies caused by the diffusion of Ti atoms in the alloy could not be replenished in time, subsequently leading to the formation of pores.

3.3. Oxidation resistance of the Al-Co-Y diffusion coating

3.3.1. Oxidation kinetics of the Al-Co-Y diffusion coating

The structure of the coatings prepared under different parameters illustrated that the Al-Co-Y diffusion coating prepared by using NaF as the activator, co-deposition temperature of 680 °C and holding time of 10 h, had a denser structure and more appropriate thickness compared to the other coatings. Thus, the coating prepared by this process was selected for high-temperature oxidation experiments, and the TiAl substrate was used as the comparison specimen. The oxidation kinetic curves of the coating and substrate in air at 950 °C are presents in Figure 8.

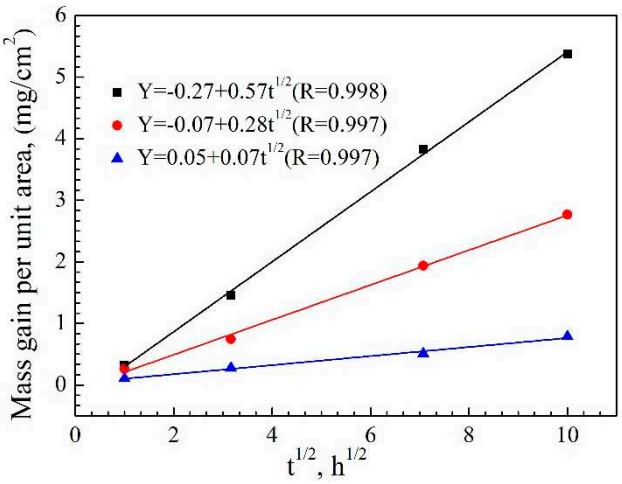

Figure 8. Oxidation kinetics of the TiAl substrate, pure Al diffusion coating and Al-Co-Y diffusion coating at 950 °C. Where y is the mass gain per unit area of the specimen (mg/cm^2), $t^{1/2}$ is the square root of the oxidation time ($h^{1/2}$), and R is the correlation coefficient of the curves.

The oxidation weight gains of the uncoated and coated specimens show approximately linear low with the square root of oxidation time, indicating that the growth of the oxide films on the specimens were controlled by diffusion. The fitted linear equations in Figure 9 reveal that the oxidation parabolic rate constant of the Al-Co-Y diffusion coating is about 4.9×10^{-3} mg^2/cm^4 h, which is lower than that of the TiAl substrate by about three orders of magnitude, and lower than that of the pure Al diffusion coating more than one order of magnitude. This clearly reveals the much better oxidation resistance of the Al-Co-Y diffusion coating than both the substrate and the pure Al diffusion coating.

Preprints (www.preprints.org) | NOT PEER-REVIEWED | Posted: 5 September 2023 doi:10.20944/preprints202309.0273.v1

3.3.2. Oxidation kinetics of the coating

Figure 9 shows the oxide scale morphology, EDS analysis maps of the scale and surface XRD pattern of the Al-Co-Y diffusion coating after oxidation at 950 ℃ for 100 h. The oxide scale was about 8 μm thick, dense, and tightly bonded to the remained coating. The EDS surface composition analysis of the oxide film shows that its composition was 10.37Ti-33.20Al-0.05Co- 3.73Nb-52.65O (at.%), in which the atomic ratio of Al to O in the dark phase was nearly 2: 3, and the atomic ratio of Ti to O in the light phase was nearly 1: 2. The above results confirm that the oxide scale was mainly composed of dark Al_2O_3 and a small amount of dispersed TiO_2.

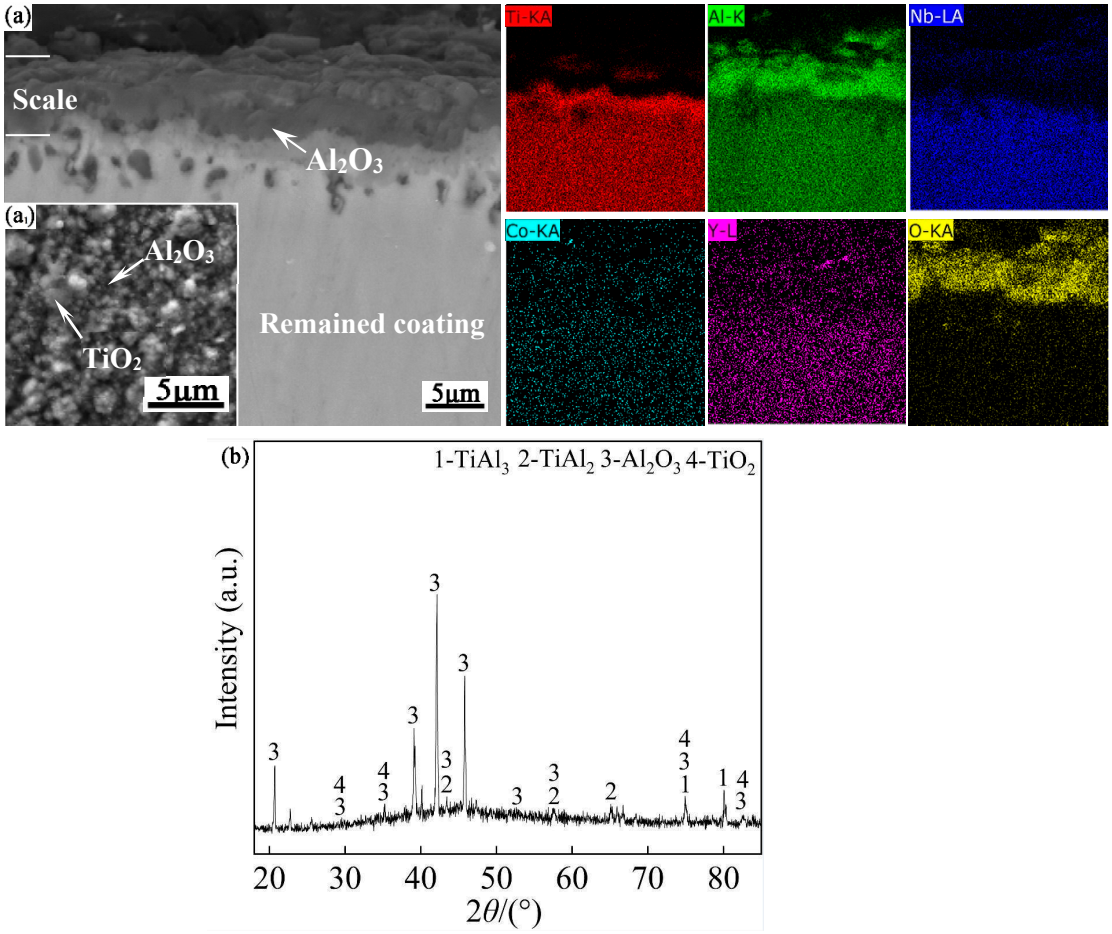

Figure 9. Surface and cross-sectional BSE morphology, the scale EDS analysis maps (a) and surface XRD pattern of the Al-Co-Y diffusion coating after oxidation for 100 h (b).

The EDS analysis maps of the scale, together with the XRD pattern in Figure 9(b) indicate that a dense Al_2O_3 layer with very small amount of TiO_2 formed in the scale, indicating that formation of the less-protective TiO_2 was effectively suppressed during oxidation. The formation of a dense, single Al_2O_3 layer can act as an effective barrier to hinder the internal diffusion of oxygen, and offer good oxidation resistance to the substrate. From the oxide scale morphology in Figure 9(a), it is also seen that after 100 h of oxidation, the remaining coating was still dense, and without any noticeable holes. This suggests that the high-temperature diffusion of permeating atoms was suppressed during the oxidation process.

4. Conclusions

Compact and well bonded Al-Co-Y diffusion coating can be prepared on TiAl alloy with using NaF as the activator at low temperature of 680 ℃. The coatings prepared with activators of NH_4Cl,

$AlCl_3$ and NaF exhibited a similar multi-layered structure, mainly composed of a $TiAl_3$ outer layer, a $TiAl_2$ inner layer, and an Al-rich TiAl inter-diffusion layer. However, intensive micro-pores formed in the coating prepared with activators NH_4Cl and $AlCl_3$.

Increasing of the co-deposition temperature in range of 650-720 °C led to a larger coating thickness but more porous coating structure. The growth of the coating exhibited a positive linear correlation between the increase in coating thickness and the square root of deposition time.

The Al-Co-Y diffusion coating prepared with by using NaF as the activator, co-deposition temperature of 680 °C and holding time of 10 h, possesses excellent high-temperature oxidation resistance. After oxidation at 950 °C for 100 h, a dense oxide scale consisting of Al_2O_3 and a small amount of TiO_2 formed on the surface of the coating. The growth of the oxide scale followed a parabolic law, and the parabolic rate constant of the oxidation weight gain was about 8.1×10^{-3} $mg^2/cm^4\ h^{1/2}$, which is lower than that of the TiAl substrate by approximately two orders of magnitude.

Author Contributions: The authors would like to express their great gratitude to Zekun Wei ,Wei Lv, Sheng Lai ,Xiaoqing Xie from Sichuan University of Science and Engineering, Yongquan Li from North Minzu University, and Fuhua Liu from Yibin Vocational and Technical College for their help in experiment testing, and Zekun Wei from Sichuan University of Science and Engineering for revision of the manuscript.

Funding: This research was financially supported by The National Natural Science Foundation of China (No. 51961003), the Major Projects of Science and Technology Department of Sichuan province (No. 22SYSX0141, 2023YFG0239), and the Project of the Key Laboratory of Mechanical Structure Optimization & Material Application Technology of Luzhou (SCHYZSA-2023-01, SCHYZSB-2023-01).

Institutional Review Board Statement: Not applicable.

Informed Consent Statement: Not applicable.

Data Availability Statement: Not applicable.

Conflicts of Interest: The authors declare no conflict of interest.

References

1. Pflumm, R.; Friedle, S.; Schütze, M. Oxidation protection of γ-TiAl-based alloys–a review. *Intermetallics*. **2015**, *56*, 1-14.[CrossRef]
2. Xiang, J.; Xie, F.; Wu, X.; et al. Aluminization of a Si-Y co-deposition coating to protect a Ti_2AlNb based alloy from high temperature oxidation. *Vacuum*.**2020**, *174*, 109190.[CrossRef]
3. Dai, J.J.; Zhang, F.Y.; Wang, A.M.; Chen, C.C.; Weng, F. Effect of Nb Doping on High Temperature Oxidation Resistance of Ti-Al Alloyed Coatings, *Journal of Materials Engineering*. **2017**, *45*, 24-31.[CrossRef]
4. Zhang, T.B.; Ding, H.; Deng, Z.H.; Zhong, H.; Hu, Y.; Xue, X.Y.; Li, J.S. Synergistic Effect of Nb and Mo on Oxidation Behavior of TiAl-Based Alloys, *Rare Metal Materials and Engineering*. **2012**, *41*, 33-37.[CrossRef]
5. Zhang, N.; Lin, J.P.; Wang, Y.L.; Yong, Z.; Chen, G.L. Influence of W, B, and Y Elements on Antioxidation of High Temperature and Long Term for TiAl Based Alloys with High Nb Content, *Rare Metal Materials and Engineering*. **2007**, *36*, 884-887.[CrossRef]
6. Song, Q.G.; L. Wang, J.; Zhu, Y.X.; Kang, J.H.; Gu, W.F.; Wang, M.C.; Liu, Z.F. Effects of Si and Y co-doping on stability and oxidation resistance of γ-TiAl based alloys, *Acta Physica Sinica*. **2019**, *68*, 196101.[CrossRef]
7. Ding, X. F.; Shen, Y.; Wang, X.M.; Tan, Y.; Wang, F.G. Influence of W, Cr on the High-temperature Oxidation Resistance of Four γ-TiAl Based Alloys with High Nb Content, *Rare Metal Materials and Engineering*. **2004**, *33*, 543-547.[CrossRef]
8. Zhou,X.; Fu, L.; Ge, H.; et al. Enhancement of tensile properties of Ti2AlNb alloy added with Ta element. *Materials Letters*. **2022**, *329*: 133233.[CrossRef]
9. Qin, Y.H.; Qiao, Y.J. The influence of the doping concentration of rare earth Ce on the structure and performance of TiAl intermetallic compound, *Journal of Functional Materials*. **2015**, *46*, 22058-22061.[CrossRef]
10. Xiang, L.L.; Zhao, L.L.; Wang, Y.L.; et al. Synergistic effect of Y and Nb on the high temperature oxidation resistance of high Nb containing TiAl alloys. *Intermetallics*. **2012**, *27*, 6-13.[CrossRef]
11. Varlese, F.A.; Tului, M.; Sabbadini, S.; et al. Optimized coating procedure for the protection of TiAl intermetallic alloy against high temperature oxidation. *Intermetallics*. **2013**, *37*, 76-82.[CrossRef]

12. Wang, P.; Li, H.; Qi, L.; et al. Synthesis of Al-TiAl$_3$ compound by reactive deposition of molten Al droplets and Ti powders. *Progress in Natural Science: Materials International.* **2011**, *21*, 153-158.[CrossRef]
13. Goral, M.; Moskal, G.; Swadzba, L. Gas phase aluminizing of TiAl intermetallics. *Intermetallics* **2009**, *17*, 669-671.[CrossRef]
14. Swadźba. R.; Bauer, P.P. Microstructure formation and high temperature oxidation behavior of Ti-Al-Cr-Y-Si coatings on TiAl. *Applied Surface Science*. **2021**, *562*: 150191. [CrossRef]
15. Laska, N.; Braun, R.; Knittel, S. Oxidation behavior of protective Ti-Al-Cr based coatings applied on the γ-TiAl alloys Ti-48-2-2 and TNM-B1. *Surface and Coatings Technology*. **2018**, *349*: 347-356.[CrossRef]
16. Anghel, E.M.; Marcu, M.; Banu, A.; et al. Microstructure and oxidation resistance of a NiCrAlY/Al_2O_3-sprayed coating on Ti-19Al-10Nb-V alloy. *Ceramics International*. **2016**, *42*, 12148-12155.[CrossRef]
17. Yang, Y.; Xiao, Q.; Ren, P.; et al. Improved oxidation resistance of γ-TiAl intermetallics by sputtered Ni+CrAlYHfSiN composite coating. *Corrosion Science.* **2021**, *187*, 109510.[CrossRef]
18. Wang W, Li J, Yuan G E, et al. Structural characteristics and high-temperature tribological behaviors of laser cladded NiCoCrAlY–B4C composite coatings on Ti6Al4V alloy. *Transactions of Nonferrous Metals Society of China*. **2021**, *31*, 2729-2739.[CrossRef]
19. Lin, H.; Liang, W.; Miao, Q.; et al. Constructing self-supplying Al_2O_3-Y_2O_3 coating for the γ-TiAl alloy with enhanced oxidation protective ability. *Applied Surface Science*.**2020**, *522*, 146439.[CrossRef]
20. Xu, Y.; Shi, P.; Cui, S.; et al. Oxidation behavior of nano-structured (Al_2O_3+ Y_2O_3)/AlY coating on γ-TiAl upon exposure to 1200° C *Ceramics International*. **2019**, *45*, 5163-5167.[CrossRef]
21. Munro T C, Gleeson B. The deposition of aluminide and silicide coatings on γ-TiAl using the halide-activated pack cementation method. *Metallurgical and Materials Transactions A*, **1996**, *27*, 3761-3772. [CrossRef]
22. Xiang, J.; Xie, F.; Wu, X.; et al. Microstructure and tribological properties of Si-Y/Al two-step deposition coating prepared on Ti_2AlNb based alloy by halide activated pack cementation technique. *Tribology International*, **2019**, *136*: 45-57. [CrossRef]
23. Brady, M.P.; Smialek, J.L.; Terepka, F. Microstructure of alumina-forming oxidation resistant Al-Ti-Cr alloys. *Scripta metallurgica et materialia*. **1995**, *32*, 1659-1664.[CrossRef]
24. Guo, M.H.; Wang, Q.M.; Gong, J.; et al. Oxidation and hot corrosion behavior of gradient NiCoCrAlYSiB coatings deposited by a combination of arc ion plating and magnetron sputtering techniques. *Corrosion Science*. **2006**, *48*, 2750-2764.[CrossRef]
25. Li, M.; Fu, L.B.; Zhang, W.L.; Sun, J.; Wang, T.G.; Jiang, S.M.; Gong, J.; Sun, C. Formation process and oxidation behavior of MCrAlY+AlSiY composite coatings on a Ni-based superalloy. *Journal of Materials Science & Technology*, 2022, 120, 65-77.[CrossRef]
26. Tang, Z.; Niewolak, L.; Shemet, V.; Singheiser, L.; Quadakkers, bW.J.; Wang, F.; Wu, W.; Gil, A. Development of oxidation resistant coatings for γ-TiAl based alloys. *Materials Science and Engineering: A*, 2002, 328(1-2): 297-301. [CrossRef]
27. Chaia, N.; Cossu, C.; Ferreira. L.M.; et al. Protective aluminide coating by pack cementation for Beta 21-S titanium alloy. *Corrosion Science*. **2019**, 160,108165.[CrossRef]
28. Huang, B.; Li, X.; Xie, X.Q.; Lai, S.; Tian, J.; Tian, W.; Liu, Z.B. High Temperature Oxidation Behavior and Failure Mechanism of Silicide Diffusion Coating Deposited on TC4 Alloy. *Rare Metal Materials and Engineering*. **2021**, *50*, 544-551.[CrossRef]
29. Xiang, Z.D.; Rose, S.R.; Datta, Packm P.K. codeposition of Al and Cr to form diffusion coatings resistant to high temperature oxidation and corrosion for γ-TiAl. *Materials science and technology*. **2002**, *18*, 1479-1484.[CrossRef]
30. Jafarian, H R.; Mirzamohammdi, S.; Rouhaghdam, A.S.; et al. Investigation of the microstructure and oxidation behavior of Cr-modified aluminide coatings on γ-TiAL alloys. *Materials Science*, **2012**, *47*, 470-475.[CrossRef]
31. Nishimoto, T.; Izumi, T.; Hayashi, S.; et al. Two-step Cr and Al diffusion coating on TiAl at high temperatures. *Intermetallics*. **2003**, *11*, 225-235.[CrossRef]
32. Li, Y.; Xie, F.; Li, X. Si-Al-Y Co-deposition Coatings Prepared on Ti-Al Alloy for Enhanced High Temperature Oxidation Resistance. *Journal of Wuhan University of Technology-Mater. Sci. Ed*. **2018**, *33*, 959-966.[CrossRef]
33. Xiang, Z.D.; Rose, S.R.; Datta, P.K. Codeposition of Al and Si to form oxidation-resistant coatings on γ-TiAl by the pack cementation process. *Materials Chemistry and Physics*. **2003**, *80*, 482-489.[CrossRef]

34. Chen, G.L.; Wang, X.T.; Ni, K.Q.; et al. Investigation on the 1000, 1150 and 1400 ℃ isothermal section of the Ti-Al-Nb system. *Intermetallics*. **1996**, *4*, 13-22.[CrossRef]
35. Xiang, Z.D.; Rose, S.R.; Burnell-Gray, J.S.; et al. Co-deposition of aluminide and silicide coatings on γ-TiAl by pack cementation process. *Journal of Materials Science*, **2003**, *38*, 19-28. [CrossRef]
36. Xiang, Z.D.; Burnell-Gray, J.S.; Datta, P.K. Aluminide coating formation on nickel-base superalloys by pack cementation process. *Journal of materials science*, **2001**, *36*, 5673-5682. [CrossRef]
37. Li, X.; Guo, X.; Qiao, Y. Friction and wear behaviors of Nb-Ti-Si-Cr based ultrahigh temperature alloy and its Zr-Y jointly modified silicide coatings. *Transactions of Nonferrous Metals Society of China*. **2016**, *26*, 1892-1901.[CrossRef]
38. Wang, X.; Li, C.; Li, M.; et al. Enhancing high-temperature oxidation resistance of Ti6Al4V alloy by simple surface aluminization. *Corrosion Science*. **2021**, 192: 109810. [CrossRef]
39. Yang, W.; Park, J.; Choi, K.; et al. Evaluation of growth kinetics of aluminide coating layers on Ti-6Al-4V alloys by pack cementation and the oxidation behaviours of the coated Ti-6Al-4V alloys. *International Journal of Refractory Metals and Hard Materials*. **2021**, 101: 105642. [CrossRef]
40. Wang, G.; Gleeson, B.; Douglass, D.L. Phenomenological treatment of multilayer growth. *Oxidation of metals*. **1989**, *31*, 415-429.[CrossRef]
41. Zhou, C.G.; Zohai, S.R.; Xu, H.B.; Kim, K.Y. Deposition of aluminide and chromium modified aluminide coatings on TiAl alloys using the halide activated pack cementation method. *Chinese Journal of Aeronautics*. **1999**, *12*, 50-57.[CrossRef]
42. Pei, Y.W.; Zhou, C.G. Improved hot corrosion resistance of Dy-Co-modified aluminide coating by pack cementation process on nickel base superalloys. *Corrosion Science*. **2016,** *112*, 710-717.[CrossRef]
43. Qi, X.; Hou, Q.; Chen, M.; et al. Microstructure and hot corrosion behavior of Al-Si-Hf coating on new γ′-strengthened cobalt-based superalloy. *Surface and Coatings Technology*. **2021**, 405: 126519. [CrossRef]